Mechanisms of equilibrium and kinetic oxygen isotope effects in synthetic aragonite at 25 °C

Sang-Tae Kim [a,*], Claude Hillaire-Marcel [b], Alfonso Mucci [a]

[a] *Earth and Planetary Sciences, McGill University, Montreal, QC, H3A 2A7, Canada*
[b] *GEOTOP, Université du Québec à Montréal, C.P. 8888, Montreal, QC, H3C 3P8, Canada*

Abstract

Aragonite was precipitated in the laboratory at 25 °C in isotopic equilibrium with Na-Ca-Mg-Cl-CO_3 solutions at two different pH values (i.e., pH = ~8.2 and ~10.8) by the constant addition method. On the basis of the oxygen isotope composition of the aragonite precipitates, it was demonstrated that the equilibrium aragonite–water fractionation factor is independent of the pH of the parent solution and equal to:

$$1000\ln\alpha_{(aragonite–H_2O)} = 29.12 \pm 0.09$$

To elucidate the mechanism(s) of aragonite precipitation, the equilibrium oxygen isotope fractionations between HCO_3^- as well as CO_3^{2-} and H_2O at 25 °C were also determined experimentally to estimate the oxygen isotope compositions of the HCO_3^- and CO_3^{2-} ions in the parent solutions. The isotopic composition of $BaCO_3$ (witherite) precipitated quantitatively from solutions of various pH values and the speciation of carbonic acid species in these solutions were combined to yield the following oxygen isotope fractionation factors:

$$1000\ln\alpha_{(HCO_3^--H_2O)} = 30.53 \pm 0.08$$

$$1000\ln\alpha_{(CO_3^{2-}-H_2O)} = 23.71 \pm 0.08$$

The oxygen isotope composition of witherite obtained from two types of fractional precipitation experiments revealed that CO_3^{2-} ions are preferentially incorporated into the growing crystal. In addition, preferential deprotonation of isotopically light HCO_3^- ions and the incorporation of the light CO_3^{2-} isotopologues are proposed to account for the kinetic isotope effects observed in the course of aragonite and witherite precipitations.
© 2006 Elsevier Inc. All rights reserved.

1. Introduction

Since McCrea (1950) reported a carbonate paleotemperature scale from his inorganically precipitated $CaCO_3$, oxygen isotope fractionation between abiogenic or biogenic calcium carbonate and water has been extensively investigated because of its application to paleoclimate research (Epstein et al., 1951, 1953; O'Neil et al., 1969; Tarutani et al., 1969; Grossman and Ku, 1986; Kim and O'Neil, 1997). Although some organisms, such as the aragonitic foraminifera *Hoeglundina elegans* (e.g., Grossman and Ku, 1986), secrete their skeletons in near oxygen isotope equilibrium with the ambient water, many others do not (e.g., McConnaughey, 1989a; Shanahan et al., 2005). For this reason, geochemists and paleoclimatologists have invested major efforts to refine and calibrate species-specific carbonate–water isotopic paleotemperature scales in order to reconstruct past environments and climate changes more accurately (e.g., Spero and Lea, 1996; Bemis et al., 1998; Owen et al., 2002b).

* Corresponding author.
  E-mail address: sangtae@eps.mcgill.ca (S.-T. Kim).

Non-equilibrium isotope effects in biogenic calcium carbonates are generally attributed to either vital and/or non-vital kinetic effect. The vital effects on oxygen isotope fractionation are directly related to the metabolic processes of a host organism or the differential composition of the internal fluids from which the mineral is precipitated (e.g., Spero and Lea, 1996; Owen et al., 2002a). Consequently, the direction and magnitude of fractionation vary from species to species because each organism has a unique calcification physiology. On the other hand, non-vital kinetic isotope effects generally discriminate against the heavier isotopes and, thus, rapidly secreted biogenic carbonates typically have lower $\delta^{18}O$ values than the expected equilibrium value. For example, McConnaughey (1989a,b) examined the carbon and oxygen isotope disequilibrium in biogenic carbonates and proposed that rapid skeletogenesis leads to a kinetic isotope effect as a result of CO_2 hydration and hydroxylation. Given that aragonitic coral skeletons are mostly precipitated from CO_2 that diffuses from the ambient water across the skeletogenic membrane .(e.g., McConnaughey, 1989a), a negative correlation between growth rate and $\delta^{18}O$ in coral skeletons reflects the non-vital kinetic isotope effect.

Non-equilibrium isotope effects in abiogenic divalent metal carbonates precipitated from aqueous bicarbonate and metal chloride solutions at low temperatures (i.e., 10, 25, and 40 °C) were recently observed (Kim and O'Neil, 1997). To explain similar observations in biogenic and synthetic carbonates, Zeebe (1999) proposed that the oxygen isotope composition of these precipitates depends on the relative abundance of the individual carbonic acid species (e.g., H_2CO_3, HCO_3^-, and CO_3^{2-}) in the parent solution at the time of precipitation and, thus, is not only a function of temperature but also of pH.

Zhou and Zheng (2002, 2003) recently reported oxygen isotope fractionation between inorganically precipitated aragonite and water at low temperatures (i.e., 0–50 °C). Although they claimed that their synthetic aragonites were formed in isotopic equilibrium, the oxygen isotope compositions of their precipitates were significantly lower than most published equilibrium values derived from inorganic and biogenic aragonites (e.g., Tarutani et al., 1969; Grossman and Ku, 1986; Böhm et al., 2000). More recently, Kim and O'Neil (2005) proposed two mechanisms of kinetic isotope fractionation that could explain why Zhou and Zheng precipitated ^{18}O-depleted synthetic aragonites. Given the discrepancies among the reported equilibrium oxygen isotope fractionation between aragonite and water and our tentative understanding of the kinetic fractionation processes at play in the $CaCO_3$–H_2O system, more systematic laboratory experiments are clearly necessary.

In this study, we not only investigated equilibrium and kinetic oxygen isotope effects in inorganically precipitated aragonites at 25 °C, but also determined the oxygen isotope fractionation factors between HCO_3^- as well as CO_3^{2-} and H_2O at 25 °C to interpret more clearly the results of the former. Our experimental results not only demonstrate,

for the first time, the pH independence of oxygen isotope fractionation in the aragonite–water system, but further elucidate the mechanisms of kinetic isotope effect and orthorhombic (i.e., witherite and aragonite) carbonate precipitation at low temperature.

2. Experimental methods

2.1. Oxygen isotope fractionation between HCO_3^- as well as CO_3^{2-} and H_2O

2.1.1. Preparation of solutions

Solutions of three different pH values (i.e., pH = ~8.3, ~10.1, and ~10.7) were prepared gravimetrically by dissolution of reagent grade $NaHCO_3$, Na_2CO_3, and a mixture of both in Nanopure (~18 MΩ cm), deionized water to the following final concentration: 5 mmolal of total dissolved inorganic carbon (DIC). These solutions were stored in a closed container and placed in a constant temperature bath (25 ± 0.01 °C) until thermal and isotopic equilibria were established (from 1 to 10 days depending on the pH of the solution). According to our investigations, oxygen isotope equilibrium among the carbonic acid species in solution is established within approximately 7 and 75 h at 25 and 10 °C, respectively, at pH = ~8.6. Our results also show that longer isotope equilibration times are required as the pH of the solution increases. These results are not presented or discussed further because very similar experimental observations were recently reported by Beck et al. (2005). Prior to the barium carbonate precipitation, an aliquot of the solution was taken for $\delta^{18}O$ analysis, and the pH of the solution was measured with a Radiometer Red-Rod™ combination pH electrode connected to a Radiometer PHM 84 pH meter. The electrode was calibrated using three NIST-traceable buffers at 25 °C (i.e., 4.01, 7.00, and 10.00).

Finally, a ~3.4 M NaOH solution was prepared from reagent grade low-carbonate NaOH pellets and CO_2 degassed (i.e., under vacuum for 1 h) deionized water. The purpose of this solution is described below.

2.1.2. Quantitative precipitations and the determination of HCO_3^- as well as CO_3^{2-}–H_2O oxygen isotope fractionation factors

After oxygen isotope equilibrium between the carbonic acid species and water was established at 25 °C, barium carbonate was quasi-instantaneously precipitated from 100 mL of the Na-CO_3 solutions. To ensure that all of the DIC in solution was precipitated, with little or no isotopic fractionation among the dissolved carbonic acid species during the precipitation, 0.05–0.25 mL of the ~3.4 M NaOH solution was added to the isotopically equilibrated 100 mL solution along with an excess (~1 g) of reagent grade $BaCl_2 \cdot 2H_2O$ powder. The addition of an excess of $CaCl_2$ always produced a mixture of three $CaCO_3$ polymorphs (i.e., calcite, aragonite, and vaterite) whereas

excess $PbCl_2$ yielded a mixture of carbonate and carbonate-chloride minerals (i.e., cerussite, hydrocerrusite, and phosgenite; Lussier, 2005). Consequently, $BaCl_2$ was selected over $CaCl_2$ and $PbCl_2$ to precipitate all the DIC as a single mineral, witherite ($BaCO_3$). The precipitation of a single mineral phase is critical to the determination of accurate $\delta^{18}O$ values and HCO_3^- or CO_3^{2-}–H_2O fractionation factors because a mineral-specific acid fractionation factor must be applied to the measured $\delta^{18}O$ of the CO_2 liberated upon acidification of the carbonate. The precipitated $BaCO_3$ was vacuum filtered through a Millipore 0.45 μm Durapore® filter membrane, and rinsed several times, first with deionized water and then with methyl alcohol. The precipitates were dried on filter paper for at least 15 h at 70–80 °C and stored in a closed vial for later isotopic analysis. The mass of $BaCO_3$ recovered from the precipitations was $100.7 \pm 1.4\%$ of the theoretical yield.

2.2. Synthesis of aragonite and witherite

2.2.1. Slow and fast precipitations of aragonite: Constant addition method

Two titrant solutions (i.e., a $NaHCO_3$ or Na_2CO_3 solution and $CaCl_2$ solution with or without Mg^{2+} depending on the pH of the experiment) were simultaneously injected at a constant and selected rate (i.e., from 0.05 to 120 mL/h) by a dual syringe pump into an air-tight Teflon® reaction vessel containing a thermally (25 ± 0.03 °C) and isotopically equilibrated Na-Mg-Cl-CO_3 or Na-Ca-Mg-Cl-CO_3 solution at a $[Mg^{2+}]/[Ca^{2+}]$ of 4:1 (see Fig. 1). The titrant and experimental solutions were prepared in Nanopure deionized water of the same oxygen isotope composition and stored immersed in a 25 ± 0.01 °C temperature bath for several days prior to each experiment to ensure isotopic equilibrium between the carbonic acid species and water. The addition of the two titrants to the experimental solution led to a supersaturation and the spontaneous nucleation of aragonite onto which crystal growth proceeded. The chemical composition of the two titrants and the starting experimental solutions were adjusted so that the pH of the experimental solution remained nearly invariant during the course of the aragonite precipitation. The experimental solution was stirred throughout the precipitation by a floating magnetic stirrer. At the beginning, during, and end of each experiment, an aliquot of the experimental solution was sampled with a plastic syringe, filtered through a Millipore 0.45 μm Durapore® syringe filter, and stored for oxygen isotope and other chemical analyses. The oxygen isotope composition of the water in the experimental solutions did not change during the course of the aragonite precipitations. The pH and temperature of the experimental solutions were monitored periodically with a digital thermometer and an Orion ROSS™ combination pH electrode calibrated using three of four NIST-traceable buffers at 25 °C (i.e., 4.00, 7.00, 10.00, and 11.00). Aragonite precipitates harvested from the experimental solution were treat-

ed like the $BaCO_3$ precipitates. The mineralogy of every run product was examined by SEM to verify whether mineral phases other than aragonite were present. The morphology of the aragonite precipitates varied from "needle-like" to "broccoli-like" depending on the experimental conditions (e.g., Morse et al., 1997; Charkrabarty and Mahapatra, 1999).

2.2.2. Quasi-instantaneous precipitations of witherite

To elucidate the mechanisms by which inorganic aragonite was precipitated from our experimental systems, various fractions of the DIC in Na-CO_3 solutions (e.g., 5, 10, and 20 mmolal) were quasi-instantaneously precipitated as witherite by varying the amount of either the NaOH solution or $BaCl_2·2H_2O$ powder added to the parent solution (see Section 2.1.2 for details). All solutions were stored as previously described in Section 2.1.1. The equivalent mass of $BaCO_3$ precipitated from these experiments varied from 3% to 91% of the DIC of the solutions.

2.3. Oxygen isotope measurements

All oxygen isotope measurements were carried out on CO_2 gas using an isotope ratio mass spectrometer at Korea University or GEOTOP-UQAM-McGill. Aragonite and witherite were analyzed at 25 °C using the classical procedure of McCrea (1950), and $\delta^{18}O$ values were normalized to the recommended values for the international reference standards NBS-18 and NBS-19 of 7.16‰ and 28.65‰ relative to VSMOW, respectively. The acid fractionation factors used in this paper are 1.01034 for aragonite (Sharma and Clayton, 1965) and 1.01063 for witherite (Kim and O'Neil, 1997). The reproducibility (1σ) of $\delta^{18}O$ measurements, based on replicate analyses of the carbonate samples, was $\pm 0.07‰$.

Water samples were analyzed by the CO_2–H_2O equilibration method at 25 °C (Cohn and Urey, 1938) at GEOTOP-UQAM-McGill or using an automated CO_2–H_2O equilibration device at Korea University. A CO_2–H_2O fractionation factor of 1.0412 (O'Neil et al., 1975) was applied to obtain the isotopic composition of the water itself, and $\delta^{18}O$ values were normalized to the oxygen isotope ratios of two laboratory standards which were directly calibrated with VSMOW and SLAP. The precision (1σ) of the water $\delta^{18}O$ analyses, on the basis of replicate analyses of the laboratory standards, was estimated at $\pm 0.05‰$.

3. Results and discussion

3.1. Overview

In order to distinguish between equilibrium and kinetic oxygen isotope effects during inorganic precipitations of aragonite in solutions at low temperatures, (1) the oxygen isotope compositions of the HCO_3^- and CO_3^{2-} ions and (2) the equilibrium oxygen isotope composition
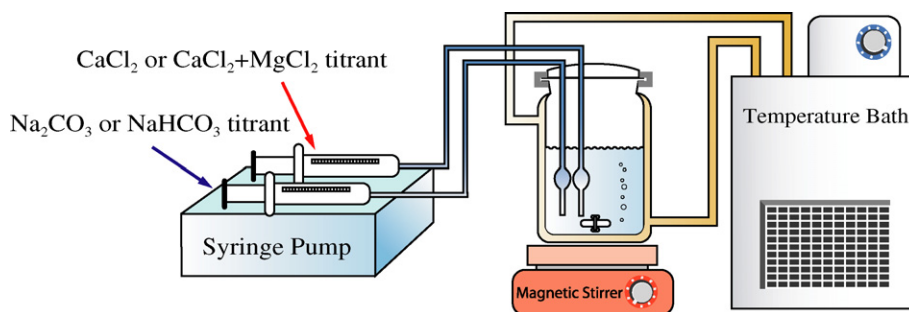
Fig. 1. A modified constant addition method system used for the synthesis of aragonite at two different pH values.

of the aragonite solid at a given temperature are required. Accordingly, the equilibrium oxygen isotope fractionation factors between HCO_3^- as well as CO_3^{2-} and H_2O at 25 °C were experimentally determined first and used to estimate the oxygen isotope compositions of HCO_3^- and CO_3^{2-} ions in our experimental solutions. Finally, the experimentally determined equilibrium oxygen isotope fractionation factor between aragonite and water at 25 °C served as a reference to identify the kinetic isotope effects associated with the fast and quasi-instantaneous precipitation experiments.

3.2. Oxygen isotope fractionations between HCO_3^- as well as CO_3^{2-} and H_2O at 25 °C

3.2.1. Carbonic acid species

The distribution of carbonic acid species in the $NaHCO_3$ or Na_2CO_3 solutions can be calculated from two of the three experimentally measurable parameters; pH, carbonate alkalinity (A_c), and total dissolved inorganic carbon (DIC) of the solution. Given the experimental design of this study (i.e., closed system to the atmosphere), the DIC concentrations and carbonate alkalinities are fixed by the amount of $NaHCO_3$ and/or Na_2CO_3 used in the preparation of the experimental solutions whereas the pH of the solutions was measured with a pH meter. Although the measured pH values do not correspond exactly to the calculated pH values (i.e., from DIC and carbonate alkalinity), the discrepancy is insignificant (i.e., maximum 0.26 pH unit, Table 1) in the context of this study. In this paper, the measured pH and gravimetric DIC values were used to calculate (Geochemist's Workbench®; Bethke, 1996, 1998) the speciation of carbonic acid species and their relative proportions to DIC. Results of these calculations are presented in Table 1. Note that the contribution of $CO_{2(aq)}$ to the DIC is maximum (~1.2%) in the lowest pH solution (5 mmolal $NaHCO_3$; pH = 8.25) and becomes almost zero in the higher pH experimental solutions. On the basis of the oxygen isotope fractionation factors reported by Beck et al. (2005), we evaluated that the error, introduced by considering $CO_{2(aq)}$ as HCO_3^- in the derivation of the oxygen isotope fractionation factors between HCO_3^- as well as CO_3^{2-} and H_2O, is of the same magni-

tude as the combined uncertainty of the conventional $\delta^{18}O$ analyses for water and carbonate (i.e., ±0.1‰). To simplify further calculations, $CO_{2(aq)}$ was treated as HCO_3^- and the relative contribution of HCO_3^- to DIC was increased accordingly.

Accepting this assumption/manipulation, four carbonic acid species are left from the initial five (i.e., DIC mass balance, Table 1). Among them, two species are ion pairs: $NaHCO_3^\circ$ and $NaCO_3^-$. The former comprises from ~0.2 to ~0.6% of the DIC and its contribution decreases with increasing pH. The latter makes up ~1.5% of the DIC at the highest pH studied (pH = 10.75) and its contribution decreases to ~0% of the DIC as pH drops to 8.25. In the recent study by Beck et al. (2005), it was shown that weak ion pairs, such as $NaCO_3^-$, have a negligible effect on the DIC-water fractionation factors at 40 °C. Even though the authors were unable to provide experimental data for temperatures lower than 40 °C, they assumed that weak ion pairs play an insignificant role in determining oxygen isotope fractionations at all the temperatures they examined (i.e., 15, 25, and 40 °C). The same assumption was applied to the current study. For this reason, the two ion pairs, $NaCO_3^-$ and $NaHCO_3^\circ$, at 25 °C are considered as CO_3^{2-} and HCO_3^-, respectively. In other words, it is assumed that the DIC in all our experimental solutions can be accounted for by only two species, HCO_3^- and CO_3^{2-}.

3.2.2. Calculating oxygen isotope fractionation factors

The measured $\alpha_{(BaCO_3-H_2O)}$ values are given in Table 2 and plotted in Fig. 2 as a function of the mole fraction of CO_3^{2-} (including $NaCO_3^-$) to DIC in the parent solutions. These results can readily be extrapolated to $[CO_3^{2-}]/DIC = 0\%$ and $[CO_3^{2-}]/DIC = 100\%$ in order to obtain the oxygen isotope fractionation factors between HCO_3^- or CO_3^{2-} and H_2O, respectively. Equilibrium oxygen isotope fractionation factors determined in this study as well as those of Beck et al. (2005) are presented in Table 3. At 25 °C, the $1000\ln\alpha_{(HCO_3^--H_2O)}$ and the $1000\ln\alpha_{(CO_3^{2-}-H_2O)}$ values obtained from this study are ~0.47‰ and ~0.48‰ smaller than those recently reported by Beck et al. (2005). However, when fractionation factors obtained from this study are recalculated by

Table 1
Calculated DIC speciation of the experimental solutions at various pH values

Solution chemistry	5 mmolal NaHCO$_3$	5 mmolal NaHCO$_3$	2.5 mmolal NaHCO$_3$ + 2.5 mmolal Na$_2$CO$_3$	5 mmolal Na$_2$CO$_3$	5 mmolal Na$_2$CO$_3$
Total DIC (Expected)	5 mmolal	5 mmolal	5 mmolal	5 mmolal	5 mmolal
pH (Measured)	8.25	8.54	10.08	10.67	10.75
pH (Calculated)	8.28	8.28	10.15	10.87	10.87
[CO$_3^{2-}$] (m)	4.91E−05	9.55E−05	2.09E−03	3.68E−03	3.85E−03
[HCO$_3^-$] (m)	4.86E−03	4.85E−03	2.85E−03	1.23E−03	1.07E−03
[NaCO$_3^-$] (m)	5.77E−07	1.12E−06	3.34E−05	7.36E−05	7.65E−05
[NaHCO$_3^{\circ}$] (m)	2.80E−05	2.79E−05	2.34E−05	1.30E−05	1.13E−05
[CO$_{2(aq)}$] (m)	5.90E−05	3.01E−05	4.99E−07	5.45E−08	3.92E−08
Total DIC (m)	5.00E−03	5.00E−03	5.00E−03	5.00E−03	5.00E−03
%[CO$_3^{2-}$]	0.98	1.91	41.85	73.66	76.94
%[HCO$_3^-$]	97.27	96.91	57.01	24.60	21.30
%[NaCO$_3^-$]	0.01	0.02	0.67	1.47	1.53
%[NaHCO$_3^{\circ}$]	0.56	0.56	0.47	0.26	0.23
%[CO$_{2(aq)}$]	1.18	0.60	0.01	0.00	0.00
%[CO$_3^{2-}$] + [NaCO$_3^-$]	0.99	1.93	42.51	75.14	78.47
%[HCO$_3^-$] + [NaHCO$_3^{\circ}$]	97.83	97.46	57.48	24.86	21.53
Total %	100.00	100.00	100.00	100.00	100.00

applying the calcite acid fractionation factor (AFF) of 1.01025, these values are statistically indistinguishable from those of Beck et al. (2005). Beck et al. (2005) did not take into account the difference in acid fractionation factors between BaCO$_3$ (i.e., witherite) and CaCO$_3$ (i.e., calcite) when calibrating their δ^{18}O$_{BaCO_3}$ values because they assumed that the difference is small ($\sim$0.13‰ at 25 °C; Kim and O'Neil, 1997). This assumption would have been acceptable if their δ^{18}O$_{BaCO_3}$ values had been corrected using the acid fractionation factor for calcite ($\alpha = 1.01050$ at 25 °C) determined by Kim and O'Neil (1997), but they corrected their measurements using the acid fractionation factor ($\alpha \approx 1.00815$ at 70 °C), a value that is the equivalent of the conventionally accepted acid fractionation factor of 1.01025 for calcite at 25 °C (i.e., Sharma and Clayton, 1965) and thus the actual discrepancy is larger ($\sim$0.38‰).

Fig. 2. Relation between $\alpha_{(witherite-H_2O)}$ and [CO$_3^{2-}$]/DIC at 25 °C. 1000ln$\alpha_{(HCO_3^--H_2O)}$ and 1000ln$\alpha_{(CO_3^{2-}-H_2O)}$ are obtained, respectively, from extrapolations to [CO$_3^{2-}$]/DIC = 0% and [CO$_3^{2-}$]/DIC = 100%.

Table 2
Experimental conditions and oxygen isotope data for quantitative precipitation experiments

Experiment ID	δ^{18}O$_{BaCO_3}$(‰)	Water ID	δ^{18}O$_{H_2O}$(‰)	$\alpha_{(BaCO_3-H_2O)}$	1000ln$\alpha_{(BaCO_3-H_2O)}$	pH	Equilibration time (h)	([CO$_3^{2-}$] + [NaCO$_3^-$])/ DIC (%)
MB-118	21.63	MGW6-3	−8.89	1.03079	30.33	8.25	246	0.99
MB-119	16.39	MGW6-3	−8.89	1.02551	25.19	10.67	246	75.14
MB-198	21.37	MGW7-2	−9.29	1.03095	30.48	8.54	2712	1.93
MB-199	21.49	MGW7-2	−9.29	1.03107	30.60	8.54	2712	1.93
MB-200	21.50	MGW7-2	−9.29	1.03108	30.61	8.54	2712	1.93
MB-202	16.14	MGW7-3	−9.29	1.02567	25.34	10.75	1512	78.47
MB-203	16.25	MGW7-3	−9.29	1.02578	25.45	10.75	1512	78.47
MB-205	16.14	MGW7-3	−9.29	1.02567	25.34	10.75	1512	78.47
MB-214	18.50	MGW7-1	−9.29	1.02805	27.66	10.08	288	42.51
MB-215	18.44	MGW7-1	−9.29	1.02799	27.61	10.08	288	42.51
MB-216	18.23	MGW7-1	−9.29	1.02778	27.40	10.08	288	42.51
MB-217	18.18	MGW7-1	−9.29	1.02773	27.35	10.08	288	42.51
MB-218	18.33	MGW7-1	−9.29	1.02788	27.50	10.08	288	42.51
MB-219	18.38	MGW7-1	−9.29	1.02793	27.55	10.08	288	42.51

Table 3
Experimentally determined fractionation factors from this and a previous study

	Temp. (°C)	$1000\ln\alpha_{(HCO_3^- - H_2O)}$	$1000\ln\alpha_{(CO_3^{2-} - H_2O)}$
This study (AFF = 1.01063)	25.0	30.53 ± 0.08	23.71 ± 0.08
This study (AFF = 1.01025)	25.0	30.90 ± 0.08	24.09 ± 0.08
Beck et al. (2005)	25.0	31.00 ± 0.15	24.19 ± 0.26

Temp., temperature; AFF, acid fractionation factor.

3.3. Oxygen isotope fractionation between aragonite and H₂O at 25 °C

3.3.1. Effect of pH

In general, temperature is the most important factor affecting the sign and magnitude of equilibrium isotope fractionations, and only one equilibrium isotope fractionation factor is expected at a given temperature. On the other hand, Zeebe (1999) proposed that the oxygen isotope composition of carbonates depends not only on the temperature of precipitation but also on the relative abundance of the isotopically distinct carbonic acid species in solution or pH at the time of precipitation. According to his hypothesis, calcium carbonate precipitated from a higher pH solution would have a lower δ^{18}O value because of a greater contribution from the isotopically lighter CO_3^{2-} ion among the carbonic acid species. This scenario, however, does not consider (1) subsequent oxygen isotope re-equilibration between the solid carbonate and the solution and (2) the specific precipitation mechanism (i.e., rate constant and reaction order with respect to each carbonic acid species) of the carbonate mineral.

To test Zeebe's (1999) hypothesis at low temperatures, aragonites were precipitated *slowly* (see Section 3.3.2 for a definition) from aqueous solutions over two distinct pH values (i.e., $pH_{ini} = 8.22 \pm 0.04$ and 10.77 ± 0.02) at 25 °C. The pH of the parent solutions was maintained within a narrow range through the addition of two titrants in equal amounts throughout the precipitations. The mixture of the two titrants reproduces the composition of the parent solutions and provides an excess of calcium and carbonate alkalinity to keep up with the CaCO₃ precipitation. The largest pH shift in a single precipitation experiment was 0.59 (see #4-Aug1604 in Table 4) but, in most cases, the variation was less than 0.2 pH unit (Fig. 3 and Table 4). The chemical composition of the titrants as well as other experimental variables, such as the duration of each experiment and the relative proportions of HCO_3^- and CO_3^{2-} to DIC in the parent solutions, are given in Tables 4 and 5.

The average $1000\ln\alpha_{(aragonite-H_2O)}$ values determined from precipitations is 29.13 ± 0.08 ($N = 6$) for pH = ∼8.2 and 29.12 ± 0.09 ($N = 8$) for pH = ∼10.8 (Fig. 3 and Table 4). These results clearly indicate that the oxygen isotope fractionation factors are, as anticipated by Deines (2005), identical within the range of pH investigated and the ana-

lytical error (±0.08 for $1000\ln\alpha_{(aragonite-H_2O)}$), irrespective of the relative contribution of the carbonic acid species to the DIC. More importantly, this observation may be interpreted as evidence that oxygen isotope equilibrium between the aragonite precipitate and water is very rapid once HCO_3^- or CO_3^{2-} are adsorbed to or incorporated into the growing aragonite crystal lattice (Reaction 1).

$$\tfrac{1}{3} CaC^{16}O_3(s) + H_2^{18}O \leftrightarrow \tfrac{1}{3} CaC^{18}O_3(s) + H_2^{16}O \quad (1)$$

Although attainment of isotopic equilibrium cannot be proven, statistically indistinguishable oxygen isotope fractionation factors, determined under distinctly different experimental conditions (i.e., pH and injection rate) in the *slow* precipitation experiments, are assumed to be representative of equilibrium values.

3.3.2. Effect of precipitation rate

The injection rate of the two titrants was varied to investigate how it influences the aragonite–water oxygen isotope fractionation factor. Given the nature of our experimental protocol (i.e., spontaneous nucleation), surface area- or weight-normalized precipitation rates cannot be readily calculated. Nevertheless, the bulk aragonite precipitation rate, following spontaneous nucleation, should be nearly proportional to the titrant injection rate at fixed titrant concentrations (Zuddas and Mucci, 1994). The surface area-normalized rate of precipitation will change as the aragonite nuclei grow, but the small deviations of the absolute precipitation rate are inconsequential to this study since 2 or 3 orders of magnitude variations in rate were investigated. The titrant injection rate is, thus, used as a proxy of the aragonite precipitation rate in the following discussion. Titrant injection rates between 0.05 and 1.0 mL/h will be referred to as *slow*, whereas higher rates will be designated as *fast*.

Over the range of the *slow* precipitation rates investigated, the oxygen isotope fractionation factor between aragonite and water is invariant, irrespective of the pH of the parent solutions (Fig. 3 and Table 4). In another set of experiments carried out at initial pHs of ∼8.2 and ∼10.7 (Table 6), the two titrants were first injected at 0.05 or 0.1 mL/h for up to 24 h during which time aragonite was nucleated, then the injection rates were abruptly increased to 96 or 120 mL/h for 2–3 h. Fig. 4 shows that the oxygen isotope fractionation factors (1000lnα) obtained from these *fast* precipitation experiments are up to 0.5 smaller than those measured from the *slow* precipitation experiments. On the basis of a Ca^{2+} mass balance calculation (e.g., #5-Apr1605 and #5-Apr2205), approximately 87% of the experimental end-product (i.e., aragonite) was precipitated during the second or *fast* stage of the experiment. Given (1) the isotopic composition of the bulk solids precipitated from these experiments (Fig. 4 and Table 6), (2) that an aragonite crystal grown during a mixed (i.e., *slow* and *fast*) precipitation rate experiment possesses a core (∼13% of the total mass) formed during the first 24 h of spontaneous

Table 4
Experimental conditions and oxygen isotope data for slow precipitation experiments

Sample	Duration (h)	Titrant 1 (mmolal)	Titrant 2 (mmolal)	Exp. solution	Inj. rate (mL/h)	Initial pH	Final pH	$\delta^{18}O_{aragonite}$ (‰)	$\delta^{18}O_{H_2O}$ (‰)	$\alpha_{(aragonite-H_2O)}$	$1000 \ln\alpha_{(aragonite-H_2O)}$
#4-Feb2504	188	3//12[a]	80/Na_2CO_3[b]	a	0.5	10.75	10.59	20.09	−9.32	1.02969	29.25
#4-Mar0604	120	3//12	80/Na_2CO_3	a	1.0	10.75	10.70	19.98	−9.36	1.02962	29.19
#4-Mar1304	143	3//12	90/Na_2CO_3	a	0.5	10.74	10.63	19.90	−9.40	1.02958	29.15
#4-July1904	278	10//0	20/$NaHCO_3$	e	0.5	8.17	8.37	19.98	−9.33	1.02959	29.16
#4-Aug0404	190	10//0	20/$NaHCO_3$	e	1.0	8.28	8.15	19.94	−9.36	1.02958	29.15
#4-Aug1604	451	10//0	20/$NaHCO_3$	e	0.1	8.20	8.79	20.03	−9.33	1.02964	29.21
#4-Nov1604	93	3//0	80/Na_2CO_3	a	0.5	10.78	10.78	19.69	−9.41	1.02938	28.95
#4-Nov2104	216	3//0	80/Na_2CO_3	a	0.5	10.78	10.71	19.79	−9.37	1.02944	29.01
#4-Feb0405	672	3//0	80/Na_2CO_3	a	0.5	10.77	10.72	19.14	−10.13	1.02957	29.14
#5-May0305	70	10//0	20/$NaHCO_3$	e	0.05/0[c]	8.18	8.49	19.13	−10.17	1.02960	29.17
#5-May2105-A	404	3//0	80/Na_2CO_3	i	0.5	10.79	10.72	19.14	−10.12	1.02956	29.13
#5-May2105-B	405	3//0	80/Na_2CO_3	i	0.5	10.79	10.74	19.15	−10.13	1.02958	29.15
#5-Jun1805-A	129	10//0	20/$NaHCO_3$	j	0.5	8.25	8.44	19.09	−10.15	1.02954	29.11
#5-Jun1805-B	129	10//0	20/$NaHCO_3$	j	0.5	8.25	8.38	19.00	−10.08	1.02938	28.95

Exp. solution, experimental solution; inj. rate, injection rate.

a, 10 mmolal Na_2CO_3 + 0.25 mmolal $CaCl_2 \cdot 2H_2O$ + 1 mmolal $MgCl_2 \cdot 6H_2O$ (initial saturation index = 1.5).
e, 10 mmolal $NaHCO_3$ + 1 mmolal $CaCl_2 \cdot 2H_2O$ + 4 mmolal $MgCl_2 \cdot 6H_2O$ (initial saturation index = 0.8).
i, 10 mmolal Na_2CO_3 + 1 mmolal $MgCl_2 \cdot 6H_2O$.
j, 10 mmolal $NaHCO_3$ + 0.15 mmolal $CaCl_2 \cdot 2H_2O$ + 1 mmolal $MgCl_2 \cdot 6H_2O$ (initial saturation index = 0.2).
[a] 3//12 denotes 3 mmolal $CaCl_2$ + 12 mmolal $MgCl_2$ solution.
[b] 80/Na_2CO_3 denotes 80 mmolal Na_2CO_3 solution.
[c] 0.05/0 denotes an injection rate change after 20 h from 0.05 to 0 mL/h.
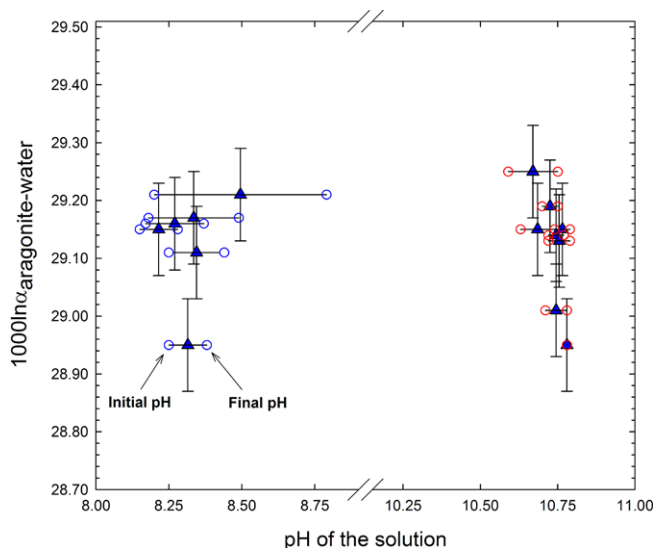
Fig. 3. Relation between $1000\ln\alpha_{(aragonite-H_2O)}$ and pH of the parent solution from the *slow* precipitation experiments at 25 °C. Vertical error bars reflect an analytical uncertainty of 0.08‰.

nucleation and *slow* precipitation stage of the experiment, and (3) assuming that the oxygen isotope composition of this core is similar to that of the *slowly* precipitated aragonites (i.e., $\delta^{18}O$ = 29.12‰; Table 4), the $1000\ln\alpha$ values for the outer rim of these aragonites (∼87% of the total mass) must be smaller than those of the bulk solids.

The observed departure from the equilibrium value could be interpreted as an inability of the adsorbed HCO_3^- and/or CO_3^{2-} or the precipitated aragonite to re-

equilibrate with the water (Reaction 1). In other words, the lifetime of a growing aragonite surface at the high precipitation rate does not allow for a complete isotopic re-equilibration with the ambient water. Interestingly, the direction of the kinetic isotope effect observed under the *fast* precipitation regime at the two different pH values is identical (Fig. 4). A detailed discussion of these observations can be found in Section 3.4.2.

3.4. Mechanism of aragonite precipitation: An oxygen isotope perspective

3.4.1. Instantaneous and fractional precipitations of $BaCO_3$ from a finite DIC reservoir

To elucidate the aragonite precipitation mechanism, the aragonite isomorph witherite was quasi-instantaneously precipitated from varying fractions of the DIC pool in iso-topically equilibrated Na-CO_3 solutions of three distinct pH values at 25 °C (see Section 2.2.2). The mole fraction (i.e., 3–91%) of the initial DIC pool precipitated as $BaCO_3$ and the oxygen isotope fractionation factors determined from the analysis of the precipitated $BaCO_3$ are presented in Table 7.

Our experiments reveal that the $\delta^{18}O$ of the $BaCO_3$ precipitated from solutions at pH = ∼10.1 and ∼10.7 remains at a value slightly smaller than that of the CO_3^{2-} ion (i.e., $\delta^{18}O$ = 23.71‰) (Fig. 5) until the fraction of DIC precipitated exceeds the mole fraction of CO_3^{2-} (including $NaCO_3^-$) in these solutions (i.e., ∼43 and ∼79% of the DIC, respectively). This experimental observation clearly demonstrates that, at high pH, CO_3^{2-} ions are preferentially incorporated into the growing witherite crystal, (i.e.,

Table 5
Calculated DIC speciation for slow precipitation experiments

pH (Measured)	8.21: Mid-pH experiment[a]		10.77: High pH experiment[b]	
Species	Molality	Mole fraction (%)	Molality	Mole fraction (%)
$[CO_{2(aq)}]$	1.15E−04	1.15	5.71E−08	0.00
$[HCO_3^-]$	9.25E−03	92.48	1.69E−03	16.89
$[NaHCO_3^\circ]$	9.19E−05	0.92	3.28E−05	0.33
$[CaHCO_3^+]$	7.53E−05	0.75	8.55E−07	0.01
$[MgHCO_3^+]$	2.08E−04	2.08	3.44E−06	0.03
$[CO_3^{2-}]$	1.06E−04	1.06	7.20E−03	72.04
$[NaCO_3^-]$	1.86E−06	0.02	2.43E−04	2.43
$[Mg_2CO_3^{2+}]$	1.44E−06	0.01	8.04E−07	0.01
$[CaCO_3^\circ]$	4.74E−05	0.47	1.94E−04	1.94
$[MgCO_3^\circ]$	1.06E−04	1.06	6.32E−04	6.32
Total DIC	1.00E−02	100.00	1.00E−02	100.00
$[CO_3^{2-}]/([HCO_3^-] + [CO_3^{2-}])$		1.13		81.01
$[HCO_3^-]/([HCO_3^-] + [CO_3^{2-}])$		98.87		18.99

[a] 10 mmolal $NaHCO_3$ + 1 mmolal $CaCl_2\cdot2H_2O$ + 4 mmolal $MgCl_2\cdot6H_2O$ solution (initial saturation index = 0.8).
[b] 10 mmolal Na_2CO_3 + 0.25 mmolal $CaCl_2\cdot2H_2O$ + 1 mmolal $MgCl_2\cdot6H_2O$ solution (initial saturation index = 1.5).

Table 6
Experimental conditions and oxygen isotope data for fast precipitation experiments

Sample	Duration (h)	Titrant 1 (mmolal)	Titrant 2 (mmolal)	Exp. solution	Inj. rate (mL/h)	Initial pH	Final pH	$\delta^{18}O_{aragonite}$ (‰)	$\delta^{18}O_{H2O}$ (‰)	$\alpha_{(aragonite–H_2O)}$	$1000ln\alpha_{(aragonite–H_2O)}$
#5-Apr1605	23	3//0[a]	80/Na_2CO_3[b]	a	0.1/96	10.74	10.94	18.55	−10.21	1.02906	28.64
#5-Apr2205	26	3//0	80/Na_2CO_3	a	0.05/96	10.73	10.87	18.60	−10.21	1.02911	28.69
#5-Oct0605	23	10//0	20/$NaHCO_3$	e	0.05/96	8.13	7.87	21.69	−7.53	1.02944	29.02
#5-Oct0905	25	10//0	20/$NaHCO_3$	e	0.05/120	8.20	8.00	21.48	−7.52	1.02922	28.80
#5-Oct2805	21	10//0	20/$NaHCO_3$	k	0.05/96	8.27	8.15	21.79	−7.55	1.02956	29.13
#5-Nov0105	25	10//0	20/$NaHCO_3$	j	0.05/96	8.39	8.11	21.71	−7.51	1.02944	29.02

Exp. solution, experimental solution; Inj. rate, injection rate.
a, 10 mmolal Na_2CO_3 + 0.25 mmolal $CaCl_2\cdot2H_2O$ + 1 mmolal $MgCl_2\cdot6H_2O$.
e, 10 mmolal $NaHCO_3$ + 1 mmolal $CaCl_2\cdot2H_2O$ + 4 mmolal $MgCl_2\cdot6H_2O$.
j, 10 mmolal $NaHCO_3$ + 0.15 mmolal $CaCl_2\cdot2H_2O$ + 1 mmolal $MgCl_2\cdot6H_2O$.
k, 10 mmolal $NaHCO_3$ + 0.3 mmolal $CaCl_2\cdot2H_2O$ + 2 mmolal $MgCl_2\cdot6H_2O$.
[a] 3//0 denotes 3 mmolal $CaCl_2$ + 0 mmolal $MgCl_2$ solution.
[b] 80/Na_2CO_3 denotes 80 mmolal Na_2CO_3 solution.
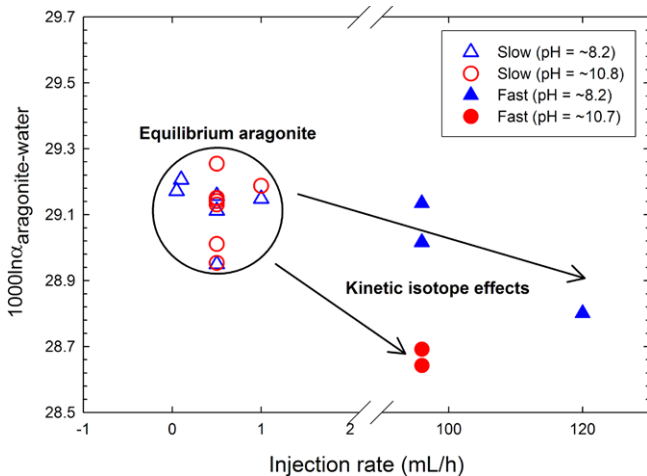
Fig. 4. Effect of injection (precipitation) rate on $1000ln\alpha_{(aragonite–H_2O)}$. Data from Tables 4 and 6 are shown.

according to Reaction 2) as opposed to other mechanisms (e.g., Reactions (3)–(5)).

$$Me^{2+} + CO_3^{2-*} \rightarrow MeCO_3^* \downarrow \qquad (2)$$

$$Me^{2+} + 2HCO_3^{-**} \rightarrow MeCO_3^{**} \downarrow + H_2CO_3 \qquad (3)$$

$$Me^{2+} + HCO_3^{-**} + OH^- \rightarrow MeCO_3^{**} \downarrow + H_2O \qquad (4)$$

$$Me^{2+} + HCO_3^{-**} \rightarrow MeCO_3^{**} \downarrow + H^+ \qquad (5)$$
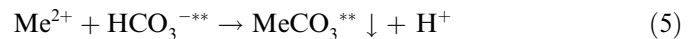
In these irreversible reactions (i.e., the solid is not allowed to back-react with the solution when the precipitation is very fast), CO_3^{2-*} and HCO_3^{-**} represent ions in oxygen isotopic equilibrium with the same water and, thus, the $\delta^{18}O$ of HCO_3^{-**} is ~6.8‰ higher than that of CO_3^{2-*} at 25 °C (Table 3 for more details). $MeCO_3^*$ and $MeCO_3^{**}$ represent a divalent metal carbonate precipitated from CO_3^{2-*} and HCO_3^{-**} ions, respectively. Under this scenario, the $\delta^{18}O$ of $MeCO_3^*$ would be at most ~6.8‰ lower than that of $MeCO_3^{**}$.

Table 7
Experimental conditions and oxygen isotope data for fractional precipitation experiments

Sample	Exp. solution (mmolal)	NaOH Soln' added	pH_{ini}	% DICpcpt	$\delta^{18}O_{witherite}$ (‰)	$\delta^{18}O_{H_2O}$ (‰)	$\alpha_{(witherite–H_2O)}$	$1000ln\alpha_{(witherite–H_2O)}$
ST-MB-51	10-NaHCO₃[b]		N/A	11	16.52	−9.30	1.02606	25.73
ST-MB-52	10-NaHCO₃		N/A	33	17.23	−9.30	1.02678	26.43
ST-MB-53	10-NaHCO₃		N/A	9	16.22	−9.30	1.02575	25.43
ST-MB-54	10-NaHCO₃		N/A	33	16.73	−9.30	1.02627	25.93
ST-MB-63	10-NaHCO₃		N/A	18	17.06	−9.30	1.02661	26.26
ST-MB-64	10-NaHCO₃		N/A	32	16.89	−9.30	1.02644	26.10
ST-MB-71	20-NaHCO₃		N/A	30	16.92	−9.33	1.02650	26.16
ST-MB-72	20-NaHCO₃		N/A	36	16.64	−9.33	1.02621	25.87
ST-MB-75	20-NaHCO₃	Yes	N/A	66	18.01	−9.33	1.02760	27.22
ST-MB-76	20-NaHCO₃	Yes	N/A	66	18.16	−9.33	1.02775	27.37
ST-MB-85	5-NaHCO₃	Yes	8.35	72	19.49	−8.89	1.02863	28.23
ST-MB-86	5-NaHCO₃	Yes	8.35	44	17.39	−8.89	1.02652	26.17
ST-MB-91	5-Na₂CO₃		10.85	91	15.68	−8.89	1.02479	24.49
ST-MB-118[a]	5-NaHCO₃	Yes	8.25	101	21.63	−8.89	1.03079	30.33
ST-MB-198[a]	5-NaHCO₃	Yes	8.54	99	21.37	−9.29	1.03095	30.48
ST-MB-199[a]	5-NaHCO₃	Yes	8.54	99	21.49	−9.29	1.03107	30.60
ST-MB-200[a]	5-NaHCO₃	Yes	8.54	100	21.50	−9.29	1.03108	30.61
ST-MB-214[a]	2.5-NaHCO₃ + 2.5-Na₂CO₃	Yes	10.08	100	18.50	−9.29	1.02805	27.66
ST-MB-215[a]	2.5-NaHCO₃ + 2.5-Na₂CO₃	Yes	10.08	100	18.44	−9.29	1.02799	27.61
ST-MB-216[a]	2.5-NaHCO₃ + 2.5-Na₂CO₃	Yes	10.08	101	18.23	−9.29	1.02778	27.40
ST-MB-217[a]	2.5-NaHCO₃ + 2.5-Na₂CO₃	Yes	10.08	101	18.18	−9.29	1.02773	27.35
ST-MB-218[a]	2.5-NaHCO₃ + 2.5-Na₂CO₃	Yes	10.08	102	18.33	−9.29	1.02788	27.50
ST-MB-219[a]	2.5-NaHCO₃ + 2.5-Na₂CO₃	Yes	10.08	101	18.38	−9.29	1.02793	27.55
ST-MB-202[a]	5-Na₂CO₃	Yes	10.75	101	16.14	−9.29	1.02567	25.34
ST-MB-203[a]	5-Na₂CO₃	Yes	10.75	100	16.25	−9.29	1.02578	25.45
ST-MB-205[a]	5-Na₂CO₃	Yes	10.75	100	16.14	−9.29	1.02567	25.34
ST-MB-119[a]	5-Na₂CO₃	Yes	10.67	105	16.39	−8.89	1.02551	25.19
ST-MB-262	5-Na₂CO₃		10.72	80	16.85	−7.54	1.02458	24.28
ST-MB-263	5-Na₂CO₃		10.72	80	16.38	−7.54	1.02410	23.82
ST-MB-264	5-Na₂CO₃		10.72	74	16.19	−7.54	1.02391	23.63
ST-MB-265	5-Na₂CO₃		10.72	31	15.99	−7.54	1.02371	23.44
ST-MB-266	5-Na₂CO₃		10.72	12	16.06	−7.54	1.02378	23.50
ST-MB-267	5-Na₂CO₃		10.72	13	16.05	−7.54	1.02377	23.49
ST-MB-268	2.5-NaHCO₃ + 2.5-Na₂CO₃		10.05	43	16.56	−7.54	1.02428	23.99
ST-MB-269	2.5-NaHCO₃ + 2.5-Na₂CO₃		10.05	48	16.90	−7.54	1.02463	24.33
ST-MB-270	2.5-NaHCO₃ + 2.5-Na₂CO₃		10.05	43	16.86	−7.54	1.02458	24.29
ST-MB-271	2.5-NaHCO₃ + 2.5-Na₂CO₃		10.05	48	16.85	−7.54	1.02458	24.28
ST-MB-272	2.5-NaHCO₃ + 2.5-Na₂CO₃		10.05	45	16.64	−7.54	1.02436	24.07
ST-MB-273	2.5-NaHCO₃ + 2.5-Na₂CO₃		10.05	29	16.10	−7.54	1.02382	23.54
ST-MB-274	10-NaHCO₃		8.28	11	18.43	−7.59	1.02622	25.88
ST-MB-275	10-NaHCO₃		8.28	3	17.99	−7.59	1.02578	25.45
ST-MB-277	10-NaHCO₃		8.28	13	18.24	−7.59	1.02603	25.69
ST-MB-280	10-NaHCO₃		8.29	13	18.24	−7.58	1.02602	25.69
ST-MB-281	10-NaHCO₃		8.29	10	18.77	−7.58	1.02655	26.20
ST-MB-282	10-NaHCO₃		8.29	5	18.11	−7.58	1.02589	25.56
ST-MB-283	10-NaHCO₃		8.29	3	17.91	−7.58	1.02568	25.36
ST-MB-284	10-NaHCO₃		8.29	3	17.80	−7.58	1.02557	25.25
ST-MB-285	2.5-NaHCO₃ + 2.5-Na₂CO₃		10.04	10	15.66	−7.55	1.02339	23.12
ST-MB-287	2.5-NaHCO₃ + 2.5-Na₂CO₃		10.04	21	15.69	−7.55	1.02342	23.15

Exp. solution, experimental solution.
% DICpcpt, % of total dissolved inorganic carbon precipitated.
[a] Denotes samples shown in Table 2.
[b] 10-NaHCO₃ denotes 10 mmolal NaHCO₃ solution.

Based on the results of their kinetic study of calcite precipitation, Zuddas and Mucci (1994) proposed that Reaction 2 is dominant for $[HCO_3^-]/[CO_3^{2-}] < 170$ and would account for more than 99% of the precipitation for $[HCO_3^-]/[CO_3^{2-}] < 70$ when calcite is precipitated from NaCl–CaCl₂ solutions. The kinetics of aragonite precipitation have not yet been investigated as thoroughly as for calcite and, thus, it could not be established whether Reactions (2)–(5) contribute equally to its precipitation or if one dominates. Nevertheless, given the kinetics of calcite precipitation described by Zuddas and Mucci (1994) and results of our witherite precipitation experiments, we
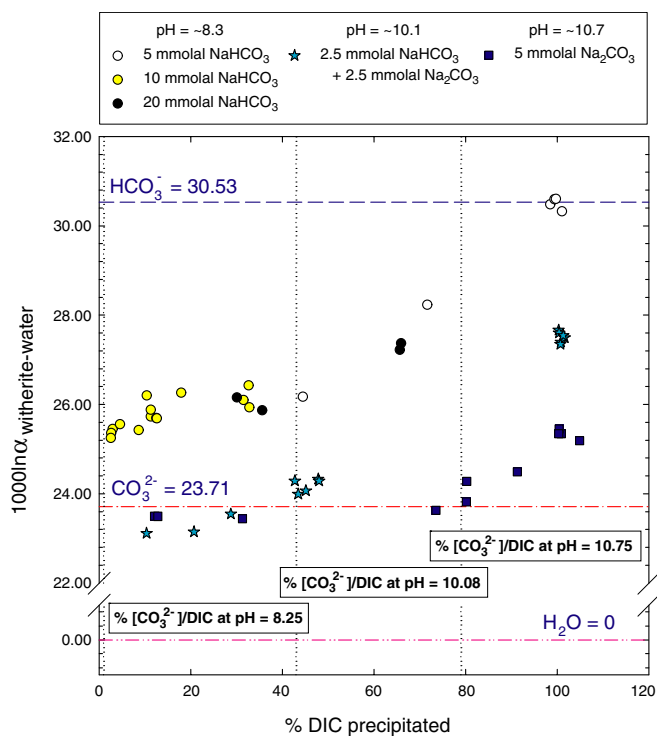
Fig. 5. Relation between $1000\ln\alpha_{(witherite–H_2O)}$ and the fraction of DIC precipitated as $BaCO_3$. This diagram demonstrates that CO_3^{2-} ions are preferentially incorporated into the solids during precipitation.

propose that Reaction 2 dominates the aragonite precipitation mechanism under conditions investigated in this study.

3.4.2. Fast and fractional precipitations of $CaCO_3$ from an infinite DIC reservoir

As indicated in Section 3.3.2, the direction of kinetic isotope effect from the two groups of *fast* precipitation experiments is identical and, thus, both yield smaller isotope fractionations or isotopically lighter aragonite (Fig. 4). These results are reproduced in Fig. 6 along with predictions based on the two precipitation models described above (Zuddas and Mucci, 1994; Zeebe, 1999). For $[CO_3^{2-}]/([HCO_3^-] + [CO_3^{2-}]) = 1.1\%$ (Fig. 6 and Table 5), the aragonite isotopic compositions predicted by Zeebe's model lie above its equilibrium value. This particular feature and the oxygen isotope composition of the aragonites obtained from the non-equilibrium (i.e., *fast*) precipitation experiments at pH = ~8.2 confirm the validity of Zuddas and Mucci's (1994) precipitation model. If Zeebe's (1999) model accounted for the mechanism of a carbonate mineral precipitation, the $\delta^{18}O$ values of the non-equilibrium carbonates would be spread between the equilibrium isotopic composition of aragonite (i.e., $\delta^{18}O = 29.12\%_0$) and the predicted value (i.e., $\delta^{18}O = 30.45\%_0$) at pH = ~8.2 (Fig. 6). In contrast, the measured $\delta^{18}O$ values of the non-equilibrium carbonates lie between the equilibrium isotopic composition of aragonite and the CO_3^{2-} ion. Thus, the results clearly establish that CO_3^{2-} ions are preferentially incorporated, relative to HCO_3^- ions, in the bulk crystal during aragonite

precipitation (i.e., Reaction 2). Fig. 6 shows how the predicted initial isotopic composition of aragonites precipitated from solutions at pH = ~8.2 and ~10.8 evolves towards the equilibrium value (i.e., $\delta^{18}O = 29.12\%_0$) as the adsorbed CO_3^{2-} or the precipitated aragonite re-equilibrates with the surrounding water (Reaction 1).

3.5. Mechanisms of kinetic isotope effect

3.5.1. Deprotonation of HCO_3^- ions in solution

Fig. 5 shows that the $BaCO_3$ solids, precipitated from a fraction (i.e., 3–91%) of the DIC pool in solutions of three distinct pH values, are depleted in ^{18}O (i.e., yield smaller oxygen isotope fractionation factors) relative to the solids formed when 100% of the DIC is quantitatively precipitated. This behavior can be attributed to the combination of two chemical reactions that lead to kinetic isotope fractionation. Given that ~97% of the DIC in the 5 mmolal NaHCO$_3$ solutions is made up of HCO_3^- ions with an ^{18}O enrichment of about 30.5‰ relative to water (see Table 1 for the other solutions) and a fraction of these ions is converted to CO_3^{2-} upon the addition of a NaOH solution (e.g., ST-MB85 and ST-MB86 in Table 7) or $BaCl_2·2H_2O$ powder (e.g., ST-MB71, ST-MB91, and ST-MB268 in Table 7), the newly formed CO_3^{2-} ions would be depleted in ^{18}O relative to their parent (i.e., HCO_3^- ions) due to preferential dissociation of lighter isotopologues (i.e., bonds to lighter isotopes are weaker than bonds to heavier isotopes) and incomplete isotope re-equilibration of newly formed CO_3^{2-} ions with water. Consequently, the $BaCO_3$ precipitated from these solutions (i.e., from the isotopically lighter CO_3^{2-} via Reaction 2 as proposed in Section 3.4) should be depleted in ^{18}O or yield smaller oxygen isotope fractionation factors, as shown in Fig. 5. Conversely, if *all* of the DIC pool is quantitatively and instantly precipitated as $BaCO_3$ such as the precipitations described in Section 3.2, the oxygen isotope composition of the resulting $BaCO_3$ should be identical to that of the initial DIC pool because no ^{18}O-enriched HCO_3^- or CO_3^{2-} reservoirs will remain. The same scenarios can be applied to interpret the isotopic composition of the other $BaCO_3$ precipitates obtained from solutions of different pH values (e.g., 5 mmolal Na_2CO_3 in Fig. 5).

3.5.2. Incorporation of CO_3^{2-} ions into a growing carbonate

To further discriminate among the kinetic isotope fractionation mechanisms associated with carbonate precipitation and on the premise that Reaction 2 dominates the carbonate precipitation mechanism, a relatively small fraction (i.e., with a minimum contribution of instantaneously deprotonated CO_3^{2-} from the HCO_3^- reservoir) of the isotopically equilibrated CO_3^{2-} ions (i.e., $\delta^{18}O = 23.71\%_0$) were precipitated as $BaCO_3$ from solutions at pH = ~10.1 and ~10.7. The $\delta^{18}O$ values of the resultant $BaCO_3$ precipitates are ~0.2‰ to ~0.6‰ smaller than the equilibrium isotopic composition of the CO_3^{2-} ion (e.g., ST-MB-267 and ST-MB-285). These results reveal that a kinetic isotope fractionation mechanism, other than the one de-
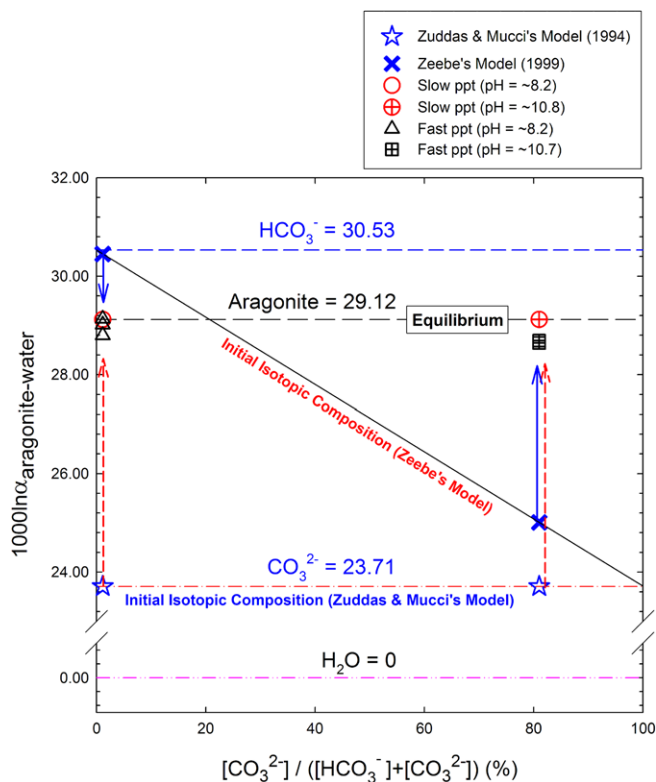
Fig. 6. A diagram showing the predicted initial isotopic composition of the precipitates based upon Zuddas and Mucci's (1994) and Zeebe's (1999) models as well as the experimentally determined oxygen isotope fractionation factors from the *slow* and *fast* aragonite precipitation experiments.

scribed in Section 3.5.1, may be at play during the carbonate mineral precipitations.

$$Me^{2+} + C^{16}O^{16}O^{16}O^{2-} \rightarrow MeC^{16}O^{16}O^{16}O \downarrow \qquad (6)$$

$$Me^{2+} + C^{16}O^{16}O^{18}O^{2-} \rightarrow MeC^{16}O^{16}O^{18}O \downarrow \qquad (7)$$

Reaction 6 is expected to be faster than Reaction 7 because lighter molecules should, according to transition state theory and Graham's Law (Criss, 1999), require a smaller activation energy (Melander and Sanunders, 1980) and diffuse faster to the reactional site. As a result, preferential incorporation of the isotopically lighter CO_3^{2-} ions among all the CO_3^{2-} isotopologues available in solution into the aragonite or witherite precipitates may account for the observed kinetic isotope fractionation that cannot be explained by the mechanism proposed in the previous section (i.e., 3.5.1).

4. Conclusions

Oxygen isotope fractionation factors between HCO_3^- as well as HCO_3^{2-} and H_2O at 25 °C were experimentally determined in order to calculate the oxygen isotope compositions of HCO_3^- and CO_3^{2-} ions in the experimental solutions used for aragonite and witherite precipitations. The $\delta^{18}O$ values of the quantitatively and quasi-instantaneously precipitated $BaCO_3$ at three distinct pH values and the

mole fractions of carbonic acid species in these solutions were combined to yield the following oxygen isotope fractionation factors at 25 °C:

$$1000\ln\alpha_{(HCO_3^- - H_2O)} = 30.53 \pm 0.08$$

$$1000\ln\alpha_{(CO_3^{2-} - H_2O)} = 23.71 \pm 0.08$$

The constant addition method was modified to synthesize equilibrium aragonite from solutions over two different pH values (i.e., pH = ~8.2 and ~10.8) at 25 °C. The measured oxygen isotope fractionation factors between aragonite and water were independent of the pH of the parent solutions. On the basis of the acid fractionation factor for aragonite (i.e., 1.01034) determined by Sharma and Clayton (1965), a new value is proposed for the oxygen isotope fractionation factor between aragonite and water at 25 °C:

$$1000\ln\alpha_{(aragonite–H_2O)} = 29.12 \pm 0.09$$

A series of $BaCO_3$ precipitation experiments was carried out from solutions of various pH values to elucidate the mechanism(s) of aragonite precipitation as well as processes leading to kinetic isotope effect during the precipitation of aragonite and witherite. Results of this study demonstrate that CO_3^{2-} ions are preferentially incorporated into the solids during precipitation. Lack of re-equilibration as a result of quick precipitation as well as preferential deprotonation of isotopically light HCO_3^- ions and the incorporation of light CO_3^{2-} isotopologues into a growing carbonate mineral are proposed to account for the kinetic isotope effects observed during carbonate mineral precipitations.

Associate editor: Thomas Chacko

References

Beck, W.C., Grossman, E.L., Morse, J.W., 2005. Experimental studies of oxygen isotope fractionation in the carbonic acid system at 15 °C, 25 °C, and 40 °C. *Geochim. Cosmochim. Acta* **69**, 3493–3503.

Bemis, B.E., Spero, H.J., Bijma, J., Lea, D.W., 1998. Reevaluation of the oxygen isotopic composition of planktonic foraminifera: experimental results and revised paleotemperature equations. *Paleoceanography* **13**, 150–160.

Bethke, C.M., 1996. *Geochemical Reaction Modeling: Concept and Applications.* Oxford University Press, New York.

Bethke, C.M., 1998. *The Geochemist's Workbench, Version 3.0: A Users Guide to Rxn, Act2, Tact, React, and Gtplot.* Hydrogeology Program, University of Illinois, Urbana.

Böhm, F., Joachimski, M.M., Dullo, W.C., Eisenhauer, A., Lehnert, H., Reitner, J., Worheide, G., 2000. Oxygen isotope fractionation in marine aragonite of coralline sponges. *Geochim. Cosmochim. Acta* **64**, 1695–1703.

Charkrabarty, D., Mahapatra, S., 1999. Aragonite crystals with unconventional morphologies. *J. Mater. Chem.* **9**, 2953–2957.

Cohn, M., Urey, H.C., 1938. Oxygen exchange reactions of organic compounds and water. *J. Am. Chem. Soc.* **60**, 679–687.

Criss, R.E., 1999. *Principles of Stable Isotope Distribution.* Oxford University Press, New York, Oxford.

Deines, P. (2005). Comment on "An explanation of the effect of seawater carbonate concentration on foraminiferal oxygen isotopes" by R.E. Zeebe, 1999. *Geochim. Cosmochim. Acta* **69**, 787–787.

Epstein, S., Buchsbaum, R., Lowenstam, H., Urey, H.C., 1951. Carbonate-water isotopic temperature scale. *Geol. Soc. Am. Bull.* **62**, 417–426.

Epstein, S., Buchsbaum, R., Lowenstam, H., Urey, H.C., 1953. Revised carbonate–water isotopic temperature scale. *Geol. Soc. Am. Bull.* **64**, 1315–1326.

Grossman, E.L., Ku, T.L., 1986. Oxygen and carbon isotope fractionation in biogenic aragonite—temperature effects. *Chem. Geol.* **59**, 59–74.

Kim, S.-T., O'Neil, J.R., 1997. Equilibrium and nonequilibrium oxygen isotope effects in synthetic carbonates. *Geochim. Cosmochim. Acta* **61**, 3461–3475.

Kim, S.-T., O'Neil, J.R. 2005. Comment on "An experimental study of oxygen isotope fractionation between inorganically precipitated aragonite and water at low temperatures, by G.-T. Zhou, Y.-F. Zheng. *Geochim. Cosmochim. Acta* **69**, 3195-3197.

Lussier, A., 2005. *The Influence of Parent-Solution Chemistry on the Precipitation of Pb-Carbonates at 25 °C, 1 Bar Total Pressure.* M.Sc. thesis, McGill University.

McConnaughey, T., 1989a. ^{13}C and ^{18}O isotopic disequilibrium in biological carbonates: I. Patterns. *Geochim. Cosmochim. Acta* **53**, 151–162.

McConnaughey, T., 1989b. ^{13}C and ^{18}O isotopic disequilibrium in biological carbonates: II. Invitro simulation of kinetic isotope effects. *Geochim. Cosmochim. Acta* **53**, 163–171.

McCrea, J.M., 1950. On the isotopic chemistry of carbonates and a paleotemperature scale. *J. Chem. Phys.* **18**, 849–853.

Melander, L., Sanunders, W.H., 1980. *Reaction Rates of Isotopic Molecules.* John Wiley & Sons, Inc., New York.

Morse, J.W., Wang, Q.W., Tsio, M.Y., 1997. Influences of temperature and Mg:Ca ratio on CaCO$_3$ precipitates from seawater. *Geology* **25**, 85–87.

O'Neil, J.R., Adami, L.H., Epstein, S., 1975. Revised value for the O^{18} fractionation between CO$_2$ and H$_2$O at 25 °C. *J. Res. US Geol. Surv.* **3**, 623–624.

O'Neil, J.R., Clayton, R.N., Mayeda, T.K., 1969. Oxygen isotope fractionation in divalent metal carbonates. *J. Chem. Phys.* **51**, 5547–5558.

Owen, R., Kennedy, H., Richardson, C., 2002a. Experimental investigation into partitioning of stable isotopes between scallop (Pecten maximus) shell calcite and sea water. *Palaeogeogr. Palaeoclimatol. Palaeoecol.* **185**, 163–174.

Owen, R., Kennedy, H., Richardson, C., 2002b. Isotopic partitioning between scallop shell calcite and seawater: Effect of shell growth rate. *Geochim. Cosmochim. Acta* **66**, 1727–1737.

Shanahan, T.M., Pigati, J.S., Dettman, D.L., Quade, J., 2005. Isotopic variability in the aragonite shells of freshwater gastropods living in springs with nearly constant temperature and isotopic composition. *Geochim. Cosmochim. Acta* **69**, 3949–3966.

Sharma, T., Clayton, R.N., 1965. Measurement of O^{18}/O^{16} ratios of total oxygen of carbonates. *Geochim. Cosmochim. Acta* **29**, 1347–1353.

Spero, H.J., Lea, D.W., 1996. Experimental determination of stable isotope variability in Globigerina bulloides: Implications for paleoceanographic reconstructions. *Mar. Micropaleontol.* **28**, 231–246.

Tarutani, T., Clayton, R.N., Mayeda, T.K., 1969. Effect of polymorphism and magnesium substitution on oxygen isotope fractionation between calcium carbonate and water. *Geochim. Cosmochim. Acta* **33**, 987–996.

Zeebe, R.E., 1999. An explanation of the effect of seawater carbonate concentration on foraminiferal oxygen isotopes. *Geochim. Cosmochim. Acta* **63**, 2001–2007.

Zhou, G.T., Zheng, Y.F., 2002. Kinetic mechanism of oxygen isotope disequilibrium in precipitated witherite and aragonite at low temperatures: An experimental study. *Geochim. Cosmochim. Acta* **66**, 63–71.

Zhou, G.T., Zheng, Y.F., 2003. An experimental study of oxygen isotope fractionation between inorganically precipitated aragonite and water at low temperatures. *Geochim. Cosmochim. Acta* **67**, 387–399.

Zuddas, P., Mucci, A., 1994. Kinetics of calcite precipitation from seawater: I.A classical chemical kinetics description for strong electrolyte solutions. *Geochim. Cosmochim. Acta* **58**, 4353–4362.